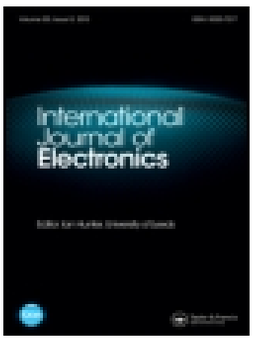

International Journal of Electronics

ISSN: (Print) (Online) Journal homepage: https://www.tandfonline.com/loi/tetn20

Full-duplex cooperative NOMA system under impacts of residual SI and MAI

Hang-Thi-Thu Nguyen , Thuy Nguyen & Xuan Nam Tran

To cite this article: Hang-Thi-Thu Nguyen , Thuy Nguyen & Xuan Nam Tran (2020): Full-duplex cooperative NOMA system under impacts of residual SI and MAI, International Journal of Electronics, DOI: 10.1080/00207217.2020.1818844

To link to this article: https://doi.org/10.1080/00207217.2020.1818844

Published online: 23 Sep 2020.

INTERNATIONAL JOURNAL OF ELECTRONICS
https://doi.org/10.1080/00207217.2020.1818844

Full-duplex cooperative NOMA system under impacts of residual SI and MAI

Hang-Thi-Thu Nguyen[a,b], Thuy Nguyen[a] and Xuan Nam Tran[b]

[a]Faculty of Information Technology, Nam Dinh University of Technology Education, Nam Dinh, Vietnam; [b]Advanced Wireless Communications Group, Faculty of Radio-Electronic Engineering, Le Quy Don Technical University, Hanoi, Vietnam

ABSTRACT

In this paper, we investigate the performance of a downlink cooperative non-orthogonal multiple access (C-NOMA) system with full-duplex decode-and-forward relaying, where a NOMA user with better channel operates as a full-duplex (FD) relay to assist other NOMA-user to forward its messages to the base station (BS). Specifically, we derive the exact expressions of the system performances in terms of outage probability and ergodic capacity for two users over the Nakagami-*m* fading channels for the case with the direct link from the BS to users. We then analyse the impacts of residual self-interference (SI) due to imperfect self-interference cancellation in the FD mode and multiple access interference (MAI) due to imperfect co-channel interference cancellation (CCIC) on the system performance. Simulation results are provided to verify the theoretical analysis and demonstrate the advantages of the FD-C-NOMA system over the FD non-cooperative NOMA (FD-NC-NOMA) system and the half-duplex C-NOMA (HD-C-NOMA) one.

ARTICLE HISTORY
Compiled 9 September 2020
Received 4 February 2020
Accepted 30 August 2020

KEYWORDS
Non-orthogonal multiple access; full-duplex relaying; decode-and-forward; cooperative communication

1. Introduction

The fifth-generation (5 G) of mobile communications is expected to meet an enormous demand in providing data services with higher transmission rate, better reliability, and larger coverage. With the dramatic growth of smart wireless devices and data traffic, there are different research directions to address the problem of radio spectrum scarcity and enhance spectral efficiency such as cognitive radio networks, spatial modulation (SM) and Index Modulation for Orthogonal Frequency Division Multiplexing (IM-OFDM) (Bagwari & Tomar, 2013; Bagwari & Tomar, 2014, 2014; Bagwari et al., 2015, 2015; Le & Tran, 2019; L. V. Nguyen et al., 2019). One of the latest techniques, non-orthogonal multiple access (NOMA) has emerged as a promising radio multiple access technique for 5 G and future wireless networks, which can satisfy requirements of massive connections and spectral efficiency (Ding et al., 2017; Higuchi & Benjebbour, 2015; Yue et al., 2017). Different from the current orthogonal multiple access (OMA) technologies, which exploit orthogonality in time or frequency domain to avoid co-channel interference, NOMA allows multiple users to share the same frequency resource at the same time, but different power levels

CONTACT Hang-Thi-Thu Nguyen thuhang.nute@gmail.com Faculty of Information Technology, Nam Dinh University of Technology Education, Nam Dinh 12000, Vietnam.

(Luo & Zhang, 2016), (Islam et al., 2017). More specifically, the NOMA scheme superposes multi-user signals at the transmitter, then separates them by means of successive interference cancellation (SIC) at the receiver. By allocating power for each user based on their channel conditions, NOMA ensures better fairness as well as increases the number of simultaneous access users. Besides, cooperative communication which allows users to collaborate with each other to forward data to the destination has been widely used in wireless systems to increase connection connectivity, transmission reliability, and link coverage (Liu et al., 2009; Amin & Lampe, 2012; Shamganth & Sibley, 2017; Li et al., 2018). Recently, cooperative non-orthogonal multiple access (C-NOMA) scheme, an integration of NOMA technology with cooperative communication, has also attracted great attention (Ding et al., 2015; Lv, Chen, & Ni, 2016; Lee, 2018; Wan et al., 2018; Kim et al., 2018). Unfortunately, user cooperation in C-NOMA results in significant reduction in the transmission rate of the relaying user due to sharing of time slots or frequencies. In addition, full-duplex (FD) communication has also been considered a promising solution for achieving high spectrum efficiency for 5 G (Chen et al., 2017; Hoang, Tan et al., 2018; Nwankwo et al., 2017; Sabharwal et al., 2014; Toka & Kucur, 2018; Z. Zhang et al., 2015). By allowing wireless terminals to transmit and receive on the same frequency and at the same time, FD communication can improve system capacity and even double the bandwidth compared with the traditional half-duplex (HD) one. For this reason, integrating FD to C-NOMA systems allows for remarkable enhancement in the system capacity and spatial diversity gain (Zhong & Zhang, 2016; Hoang, Van Son et al., 2018; X.-X. Nguyen & Do, 2019; Chu & Zepernick, 2018; Z. Zhang, Ma, Xiao, Ding, & Fan, 2017; Yue et al., 2018; L. L. Zhang et al., 2017). In general, the cooperative full-duplex modes can be implemented by cooperating network relays (Zhong & Zhang, 2016; Hoang, Van Son et al., 2018; Chu & Zepernick, 2018; X.-X. Nguyen & Do, 2019) or users (Z. Zhang et al., 2017; Yue et al., 2018; L. L. Zhang et al., 2017). In (Zhong & Zhang, 2016), the authors proposed a NOMA system with an FD relay assisting data transmission to two far users and derived the outage probability and ergodic sum capacity expressions for it under the complex Gaussian channels. Similar to the model in (Zhong & Zhang, 2016), but generalised to the Nakagami-*m* channel, (Hoang, Van Son et al., 2018) calculated the exact expressions of the outage probability and optimised power allocation coefficient for a system with energy harvesting relaying node while paper (Chu & Zepernick, 2018) analyses the outage performance and sum rate of the NOMA system with perfect SIC. The work in (X.-X. Nguyen & Do, 2019) derived the analytical expression of energy efficiency and compared outage performance of an FD-C-NOMA system with that of the HD one. In other works (Z. Zhang et al., 2017; Yue et al., 2018), the authors applied FD to a device-to-device (D2D) system and analysed its performances in the case of having a dedicated HD and FD relay over the Rayleigh fading channels. The work (L. L. Zhang et al., 2017) optimises the NOMA downlink system with full-duplex relaying.

Although the adoption of the relay for a full-duplex transmission system helps to improve its stability, future wireless networks require fast and flexible configuration without prior complicated infrastructure setup. Thus, the user-to-user cooperation model is a favourite solution. As a result, the C-NOMA system in which a strong user with better channel gain acts as an FD relaying node to forward data of a weak user, i.e. with worse channels, is worth investigation. With this motivation, in this paper, we conduct a thorough study on the FD-C-NOMA system under the realistic system and

channel conditions. Against the previous works, the main contributions of the paper are summarised as follows:

• We analyse a general FD-C-NOMA system under the impact of the Nakagami-*m* channel. Different from the previous works, our system is more realistic as it includes the imperfect interference cancellation due to both FD and NOMA implementation. The system thus suffers simultaneously from both residual self-interference (SI) due to the FD mode and residual co-channel interference (CCI) due to multiple access, i.e. MAI, at the relay node. The residual SI is modelled as a Rayleigh random variable instead of a Gaussian one.

• We derive the closed-form expressions of the outage probability and the ergodic capacity for each user taking into account the influence of the residual SI and MAI factors so that we can use them for designing practical systems. These derived expressions are then used to evaluate performance of the system numerically against the FD non-cooperative NOMA (FD-NC-NOMA) and HD-C-NOMA.

The remainder of this paper is organised as follows: Section II describes the system model of the considered C-NOMA system. Section III presents detailed analysis of the system performance in terms of outage probability and ergodic capacity. Section IV represents numerical results and performance evaluation. Finally, conclusions are drawn in Section V.

2. System Model

Let us consider a downlink C-NOMA system with a base station (BS) that transmits the superposed signal to two single-antenna users (UE_1, UE_2) as illustrated in Figure 1. Without loss of generality, we assume that the gain of the channel between BS and UE_1 is higher than that corresponding to UE_2, i.e. $|h_1|^2 > |h_0|^2$. UE_1 serves as a decode-and-forward (DF) relay in the FD mode to forward the received signal from BS to UE_2 while receiving the transmitted signal from BS simultaneously. At UE_2, the signals from the direct link and the relay link are combined using the selection combining (SC) technique and then separated by SIC to retrieve its signal. We assume that the BS total power P_t is divided to UE_1 and UE_2 by the power allocation coefficients a_1, a_2, respectively. According to the NOMA principle, a_i is subject to the constraints $a_1 + a_2 = 1$ and $a_1 < a_2$. All

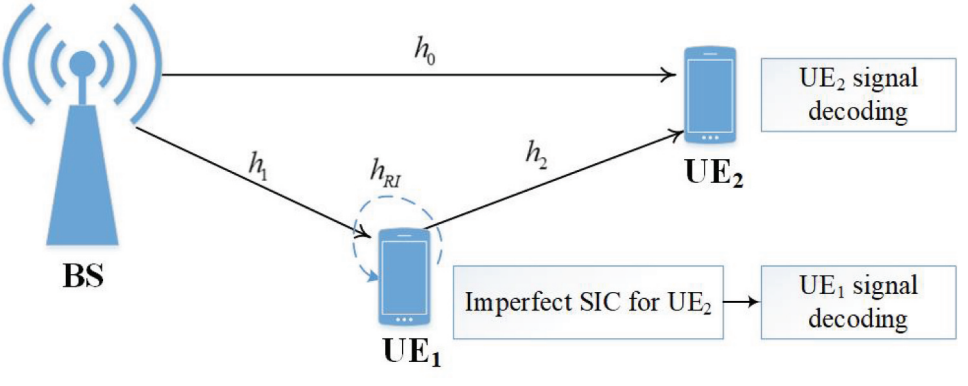

Figure 1. FD-C-NOMA system model.

channels between BS and UE_2, BS and UE_1, and UE_1 and UE_2 are assumed to undergo flat and independent and identically distributed (i.i.d) Nakagami-*m* fading with the complex channel coefficients h_0, h_1, h_2 respectively. Besides, in order to make the FD communications possible, SI needs to be cancelled effectively and three interference cancellation schemes can be used together in the space (propagation) domain, analogue domain and digital domain (Sabharwal et al., 2014; Z. Zhang et al., 2015). The works (Bharadia et al., 2013; Nwankwo et al., 2017) report an attenuation level of up to 50 dB in the propagation domain if possible solutions are used. The impact of the SI channel is thus mainly due to the reflected paths. In this case, the channel gain of the direct path is no longer dominant compared with the reflected paths. Since the direct and reflected paths are statistically independent, using the central limit theorem, the overall path gain of the SI channel can be well described by a complex Gaussian variable with its magnitude, denoted by $|h_{\mathrm{RI}}|$, having Rayleigh distribution (Hoang, Van Son et al., 2018; Yue et al., 2018).

Let x_i denote the signals of $UE_i, i = 1, 2$ with $\mathrm{E}\{|x_i|^2\} = 1$; $\mathrm{E}\{.\}$ denotes the expectation operation. In the NOMA downlink system, a superposed signal $s(t) = \sqrt{a_1 P_t}x_1(t) + \sqrt{a_2 P_t}x_2(t)$ is transmitted from BS to the two users. The received signal at UE_1 is expressed as

$$y_1(t) = h_1\left(\sqrt{a_1 P_t}x_1(t) + \sqrt{a_2 P_t}x_2(t)\right) + h_{\mathrm{RI}}\sqrt{P_r}\tilde{x}_1(t) + n_1(t), \tag{1}$$

where $\tilde{x}_1(t)$ is the forwarding signal from UE_1 to UE_2 and P_r is the transmit power of UE_1. For simplicity, we assume that $P_t = P_r = P$ and define $\rho = \frac{P}{\sigma_n^2}$ as the signal-to-noise (SNR) ratio; $n_1(t)$ denotes the additive white Gaussian noise (AWGN) at UE_1, with zero-mean and variance σ^2, i.e. $n_1 \sim \mathcal{CN}(0, \sigma^2)$. UE_1 first decodes the superior signal x_2 and then removes it from the received signal to detect x_1. Thus, the signal-to-interference-plus-noise-ratio (SINR) to decode x_2 at UE_1 is given by

$$\gamma_{12} = \frac{|h_1|^2 a_2 \rho}{|h_1|^2 a_1 \rho + |h_{\mathrm{RI}}|^2 \rho + 1}. \tag{2}$$

The SINR for detecting x_1 is given by

$$\gamma_{11} = \frac{|h_1|^2 a_1 \rho}{|h_1|^2 a_2 \varepsilon \rho + |h_{\mathrm{RI}}|^2 \rho + 1}, \tag{3}$$

where $0 \leq \varepsilon \leq 1$ is the residual power factor after SIC. When $0 \leq \varepsilon \leq 1$, SIC at UE_1 is imperfect; otherwise, it is perfect. After decoding successfully, UE_1 forwards x_2 to UE_2. The received signals of the direct link and the relay link at UE_2 are, respectively, expressed as follows

$$y_{2S}(t) = h_0\left(\sqrt{a_1 P_t}x_1(t) + \sqrt{a_2 P_t}x_2(t)\right) + n_{2S}(t), \tag{4}$$

$$y_{2R}(t) = h_2\sqrt{P_r}x_2(t - \tau) + n_{2R}(t), \tag{5}$$

where τ is the processing delay. SINRs of the direct link and the relay link at UE_2 denoted, respectively, by γ_{2R}, can be determined as follows

$$\gamma_{2S} = \frac{|h_0|^2 a_2 \rho}{|h_0|^2 a_1 \rho + 1}, \tag{6}$$

$$\gamma_{2R} = |h_2|^2 \rho. \tag{7}$$

3. Performance Analysis

In this section, we analyse two important system performance parameters, i.e. outage probability and ergodic capacity, and derive their closed-form expressions for numerical calculations.

3.1. Outage probability

3.1.1. Outage probability of UE_1

Let γ_{thi} be a required SINR threshold for acceptable performance and $\gamma_{thi} = 2^{R_i} - 1$, where R_i is the target transmission rate of user UE_i, $i = 1, 2$. The outage event for relaying system happens when the achieved SINR for detecting x_i is smaller than the SINR threshold. In contrast, the success event for relaying system occurs when UE_1 successfully decodes x_2 and is able to decode its own data, x_1. Hence, the outage probability of UE_1 can be deduced as follows (Yue et al., 2018, Equation(9)):

$$\mathrm{OP}_1 = 1 - \Pr(\gamma_{12} > \gamma_{\mathrm{th2}}, \gamma_{11} > \gamma_{\mathrm{th1}}). \tag{8}$$

The outage probability of UE_1 can be calculated by Theorem 1.

Theorem 1

The closed-form expression of the outage probability for the relay UE_1 is given by

$$\mathrm{OP}_1 = \begin{cases} 1, & \frac{a_1}{a_2} \geq \frac{1}{\gamma_{\mathrm{th2}}} \text{ or } \frac{a_1}{a_2} \leq \varepsilon\gamma_{\mathrm{th1}} \\ F(b_1), & \varepsilon\gamma_{\mathrm{th1}} \leq \frac{a_1}{a_2} \leq \frac{\gamma_{\mathrm{th1}}(1+\varepsilon\gamma_{\mathrm{th2}})}{\gamma_{\mathrm{th2}}(1+\gamma_{\mathrm{th1}})} \\ F(b_2), & \frac{\gamma_{th1}(1+\varepsilon\gamma_{th2})}{\gamma_{th2}(1+\gamma_{th1})} \leq \frac{a_1}{a_2} \leq \frac{1}{\gamma_{th2}} \end{cases} \tag{9}$$

where $F(b_i)$ is a function of b_i with $i = 1, 2$ and $b_1 = \frac{m_1\gamma_{\mathrm{th1}}}{\Omega_1\rho(a_1 - a_2\varepsilon\gamma_{\mathrm{th1}})}$, $b_2 = \frac{m_1\gamma_{\mathrm{th2}}}{\Omega_1\rho(a_2 - a_1\gamma_{\mathrm{th2}})}$. $F(b_i)$ is defined as

$$F(b_i) = 1 - \frac{1}{\Omega_{\mathrm{RI}}} e^{-b_i} \times \sum_{k=0}^{m_1-1} \sum_{t=0}^{k} \frac{b_i^k}{k!} \binom{k}{t} \rho^t t! \left(b_i\rho + \frac{1}{\Omega_{\mathrm{RI}}}\right)^{-t-1}, \tag{10}$$

where $\Omega_{\mathrm{RI}} = E\{|h_{\mathrm{RI}}|^2\}$ is average channel gain of self-interference channel.

3.1.2. Outage probability of UE_2

We define the outage event of UE_2 is that the received SINR after SC at UE_2 is less than its SINR target. Based on the definition of outage probability in (Goldsmith, 2005, eq.(6.46)), the outage probability of UE_2 is expressed as

$$\mathrm{OP}_2 = \Pr\left(\gamma_2^{\mathrm{SC}} \leq \gamma_{\mathrm{th2}}\right), \tag{11}$$

where γ_2^{SC} is the output SINR at the SC combiner output and can be inferred from (Goldsmith, 2005, sect.(7.2.2)) and expressed as

$$\gamma_2^{SC} = \max\{\min(\gamma_{12}, \gamma_{2R}), \gamma_{2S}\}. \tag{12}$$

The exact expression of the outage probability of UE_2 can be obtained using the following theorem.

Theorem 2

The closed-form expression of the outage probability for UE_2 is given by

$$\mathrm{OP}_1 = \begin{cases} 1, & \frac{a_1}{a_2} \geq \frac{1}{\gamma_{th2}} \text{ or } \frac{a_1}{a_2} \leq \in\gamma_{th1} \\ F(b_1), & \in\gamma_{th1} \leq \frac{a_1}{a_2} \leq \frac{\gamma_{th1}(1+\in\gamma_{th2})}{\gamma_{th2}(1+\gamma_{th1})} \\ F(b_2), & \frac{\gamma_{th1}(1+\in\gamma_{th2})}{\gamma_{th2}(1+\gamma_{th1})} \leq \frac{a_1}{a_2} \leq \frac{1}{\gamma_{th2}} \end{cases} \tag{13}$$

where $\beta = \frac{\gamma_{th2}}{\rho(a_2 - a_1\gamma_{th2})}$.

Proof. See Appendix B □

3.2. Ergodic capacity

3.2.1. Ergodic capacity of UE_1

At the relay node, the achievable rate of UE_1 is written as $C_1 = \log(1+\gamma_{11})$, so the ergodic capacity of UE_1 can be derived as (Goldsmith, 2005):

$$\bar{C}_1 = \mathrm{E}\left[\log\left(1 + \frac{|h_1|^2 a_1 \rho}{|h_1|^2 a_2 \varepsilon\rho + |h_{\mathrm{RI}}|^2 \rho + 1}\right)\right]. \tag{14}$$

The following theorem provides the expression for ergodic capacity $\bar{C}_1$.

Theorem 3 The ergodic capacity of UE_1 is given by

$$\bar{C}_1 = \frac{1}{\ln 2}(\mathrm{I}_1 - \mathrm{I}_2), \tag{15}$$

where

$$\mathrm{I}_i = \begin{cases} \frac{1}{\Omega_{\mathrm{RI}}} \sum_{k=0}^{m_1-1} \sum_{t=0}^{k} \frac{b_{1i}^k}{k!} \binom{k}{t} \frac{(-1)^t \rho^t t!}{c_{1i}^{t+1}} \left(\mathrm{e}^{b_{1i}} \right. \\ \left. \times \Gamma(k-t+1)\Gamma(t-k, b_{1i}) - \mathrm{I}_{1i}\right) + \Delta, \quad c_{1i} \neq 0 \\ \frac{1}{\Omega_{\mathrm{RI}}} \sum_{k=0}^{m_1-1} \sum_{t=0}^{k} \frac{b_{1i}^k}{k!} \binom{k}{t} \frac{(-1)^t}{(t+1)\rho} \\ \times \left(\mathrm{e}^{b_{1i}} \Gamma(k+2)\Gamma(-1-k, b_{1i})\right) + \Delta, \quad c_{1i} = 0 \end{cases} \tag{16}$$

and $i = 1, 2$,

$$\mathrm{I}_{1i} = \sum_{m=0}^{t} \left(\frac{c_{1i}}{\rho}\right)^m \frac{\mathrm{e}^{d_{1i}}(k+m-t)!\Gamma(t-k-m, d_{1i})}{m!}, \tag{17}$$

where $b_{11} = \frac{m_1}{\Omega_1\rho(a_1+\varepsilon a_2)}$, $c_{11} = -\frac{m_1}{\Omega_1(a_1+\varepsilon a_2)} + \frac{1}{\Omega_{\mathrm{RI}}}$, $b_{12} = \frac{m_1}{\Omega_1\rho\varepsilon a_2}$, $c_{12} = -\frac{m_1}{\Omega_1\varepsilon a_2} + \frac{1}{\Omega_{\mathrm{RI}}}$, $d_{1i} = b_{1i} + \frac{c_{1i}}{\rho}$, $\Delta = -e^{\frac{1}{\rho\Omega_{\mathrm{RI}}}}\mathrm{E}_i\left(-\frac{1}{\rho\Omega_{\mathrm{RI}}}\right)$ (Gradshteyn & Ryzhik, 2014, eq.(3.352.4)).

Proof. See Appendix C□

3.2.2. Ergodic capacity of UE_2

The derivation of the achievable capacity of UE_2 can be possible by using the expression: $C_1 = \log\left(1+\gamma_2^{SC}\right)$. However, it is difficult to derive the closed-form as well as the high SNR approximation for the expression of ergodic capacity for UE_2. Obviously, UE_2 receives data from BS and the relay, so the ergodic capacity for UE_2 can be defined as $\bar{C}_2 \triangleq \max\left(\bar{C}_{2S}, \bar{C}_{2R}\right)$, where $\bar{C}_{2S}$, $\bar{C}_{2R}$ are the ergodic capacity of the direct link and the relay link between BS and UE_2. Moreover, $\bar{C}_{2R}$ is dominated by the minimum of the capacities of the channels from BS to UE_1 and from UE_1 to UE_2 for x_2, which are, respectively, denoted by $\bar{C}_{1S}^{x_2}, \bar{C}_{12}^{x_2}$. Hence, the ergodic capacity of UE_2 is obtained as

$$\bar{C}_2 \triangleq \max\left\{\bar{C}_{2S}, \min\left(\bar{C}_{1S}^{x_2}, \bar{C}_{12}^{x_2}\right)\right\}. \tag{18}$$

The sub ergodic capacity in (18) needs to be clearly determined to get the expression of $\bar{C}_2$. First of all, C_{1S} can be computed by the following theorem.

Theorem 4 The ergodic capacity $\bar{C}_{1S}$ can be given by

$$\bar{C}_{1S}^{x_2} = \frac{1}{\ln 2}\left(\mathrm{Q}_1 - \mathrm{Q}_2\right), \tag{19}$$

where

$$\mathrm{Q}_i = \begin{cases} \frac{1}{\Omega_{\mathrm{RI}}} \sum\limits_{k=0}^{m_1-1} \sum\limits_{t=0}^{k} \frac{b_{2i}^k}{k!} \binom{k}{t} \frac{(-1)^t \rho^t t!}{c_{2i}^{t+1}} \\ \times\left(\mathrm{e}^{b_{2i}} \Gamma(k-t+1)\Gamma(t-k, b_{2i}) - \mathrm{Q}_{2i}\right) + \Delta, \quad c_{2i} \neq 0 \\ \frac{1}{\Omega_{\mathrm{RI}}} \sum\limits_{k=0}^{m_1-1} \sum\limits_{t=0}^{k} \frac{b_{2i}^k}{k!} \binom{k}{t} \frac{(-1)^t}{(t+1)\rho} \\ \times\left(\mathrm{e}^{b_{2i}} \Gamma(k+2)\Gamma(-1-k, b_{2i})\right) + \Delta, \qquad c_{2i} = 0 \end{cases} \tag{20}$$

and $i = 1, 2$,

$$\Theta_{2i} = \sum_{p=0}^{t} \left(\frac{c_{2i}}{\rho}\right)^m \frac{e^{d_{2i}}(k+p-t+1)!\Gamma(t-k-p, d_{2i})}{p!}, \tag{21}$$

where $b_{21} = \frac{m_1}{\Omega_1 \rho(a_1+a_2)}$, $c_{11} = -\frac{m_1}{\Omega_1(a_1+a_2)} + \frac{1}{\Omega_{\mathrm{RI}}}$, $b_{22} = \frac{m_1}{\Omega_1 \rho a_1}$, $c_{22} = -\frac{m_1}{\Omega_1 \rho a} + \frac{1}{\Omega_{\mathrm{RI}}}$, $d_{2i} = b_{2i} + \frac{c_{2i}}{\rho}$, $\Delta = -e^{\frac{1}{\rho\Omega_{\mathrm{RI}}}} \mathrm{E}_i\left(-\frac{1}{\rho\Omega_{\mathrm{RI}}}\right)$.

Proof. The ergodic capacity of UE_1 which is derived from the expression of achievable rate $C_{1S}^{x_2} = \log(1+\gamma_{12})$ can be written as□

$$\bar{C}_{1S}^{x_2} = \mathrm{E}\left[\log\left(1 + \frac{|h_1|^2 a_2 \rho}{|h_1|^2 a_1 \rho + |h_{\mathrm{RI}}|^2 \rho + 1}\right)\right]. \tag{22}$$

Similarly to the case of Theorem 3, we can obtain the result in (20).

Next, we analyse the rest of the expression (18).

Note that $\bar{C}_{12}^{x_2}$ can be expressed as (Yue et al., 2018, Equation(33)):

$$\bar{C}_{12}^{x_2} = \mathrm{E}\left[\log\left(1+|h_2|^2\rho\right)\right]$$

$$= \frac{1}{\ln 2}\int_0^{\infty}\frac{1-F_W(w)}{1+w}dw, \tag{23}$$

where $F_W(w)$ is the CDF of $W = |h_2|^2\rho$ which has the Gamma distribution since the complex channel coefficient h_2 is an i.i.d Nakagami-m distributed random variable. Using (Shankar, 2017), it can be expressed as follows

$$F_W(w) = 1 - e^{-\frac{m_2 w}{\Omega_2\rho}}\sum_{k=0}^{m_2-1}\left(\frac{m_2 w}{\Omega_2\rho}\right)^k\frac{1}{k!}. \tag{24}$$

Substituting (24) into (23) and after some manipulations, the ergodic capacity can be given by

$$\bar{C}_{12}^{x_2} = \frac{1}{\ln 2}\sum_{k=0}^{m_2-1}\frac{m_2}{\Omega_2\rho}e^{\frac{m_2}{\Omega_2\rho}}\Gamma\left(-k,\frac{m_2}{\Omega_2\rho}\right). \tag{25}$$

The ergodic capacity of the direct link from BS to UE_2 can be written as

$$\bar{C}_{2S} = \mathrm{E}\left[\log\left(1+\frac{|h_0|^2 a_2\rho}{|h_0|^2 a_1\rho+1}\right)\right]$$

$$= \mathrm{E}\left[\log\left(1+|h_0|^2(a_1+a_2)\rho\right)\right] - \mathrm{E}\left[\log\left(1+|h_0|^2 a_1\rho\right)\right] \tag{26}$$

$$= \frac{1}{\ln 2}\left(\int_0^{\infty}\frac{1-F_U(u)}{1+u}du - \int_0^{\infty}\frac{1-F_V(v)}{1+v}dv\right), \tag{27}$$

where $U = |h_0|^2(a_1+a_2)\rho$, $V = |h_0|^2 a_1\rho$. $F_U(u)$, $F_V(v)$ the CDF of U, V. Similar to the $F_W(w)$ expression, they expressed as

$$F_U(u) = 1 - e^{-\frac{m_0 u}{\Omega_0(a_1+a_2)\rho}}\sum_{k=0}^{m_2-1}\left(\frac{m_0 u}{\Omega_0(a_1+a_2)\rho}\right)^k\frac{1}{k!}, \tag{28}$$

$$F_V(v) = 1 - e^{-\frac{m_0 v}{\Omega_0 a_1\rho}}\sum_{k=0}^{m_2-1}\left(\frac{m_0 v}{\Omega_0 a_1\rho}\right)^k\frac{1}{k!}. \tag{29}$$

Let $b_{01} = \frac{m_0 u}{\Omega_0(a_1+a_2)\rho}$, $b_{02} = \frac{m_0 v}{\Omega_0 a_1\rho}$. Substituting (28) and (29) into (27) and using (Gradshteyn & Ryzhik, 2014, eq.(3.383.10)) we get the following result

$$\bar{C}_{2S} = \frac{1}{\ln 2}\left[\sum_{k=0}^{m_0-1} b_{01}\mathrm{e}^{b_{01}}\Gamma(-k,b_{01}) - \sum_{k=0}^{m_0-1} b_{02}\mathrm{e}^{b_{02}}\Gamma(-k,b_{02})\right]. \tag{30}$$

Note that, due to properties of the OP and capacity expressions, the approximation of these functions under extreme conditions results in large errors. Therefore, further asymptotic analysis of the OP and capacity is skipped here.

4. Performance Evaluations

In this section, we evaluate performances of FD-C-NOMA system using numerical results and compare them with those of FD-NC-NOMA and HD-C-NOMA systems. Simulation results are also provided to validate the theoretical analysis. Unless otherwise specified, the parameters used for evaluations are illustrated in Table 1.

In Figure 2, the outage probabilities of UE_1 and UE_2 are evaluated for $\Omega_{RI} = \{-15, -20, -30\}$ (dB). Note from the figure that the outage probability curves obtained by numerical calculations using Theorem 1 and Theorem 2 match well with those by Monte-Carlo simulations, which validates our analysis. It is noteworthy that there is a strong influence of the SI on the outage performance of the system, especially in the high SNR region. Due to the residual SI at UE_1, the outage probability curves of UE_1 exhibit saturation in the high E_b/N_0 regime while this is not seen in the UE_2 ones. It also makes the performance of the relay node seriously decline by more than half at the value of $\Omega_{RI} = -15$ (dB) compared to $\Omega_{RI} = -30$ (dB). On the other hand, the outage probability of UE_2 improves significantly since the received signals from two links are combined, which provides spatial diversity gain.

Figure 3 shows the effect of ε on the system outage performance where ε is chosen as $\{0.01, 0.1, 0.4\}$. Obviously, the outage performance of UE_2 is constant whereas the one of UE_1 is significantly declined, especially in the case of $\varepsilon > 0.1$. With the imperfect SIC system, where UE_1 cannot completely subtract the signal of UE_2 by SIC, the error is propagated at UE_1 but not to UE_2. Therefore, this does not affect detection of the UE_2's

Table 1. Simulation parameters.

Parameters	Value
Power allocation coefficients	$a_1 = 0.3,\ a_2 = 0.7$
Target rates	1 bpcu
Channel gains	$\Omega_0 = 1, \Omega_1 = 2, \Omega_2 = 1$
Imperfect SIC	0.01
Residual self-interference	−20 dB
Nakagami multipath fading parameter	$m_1 = m_2 = m_3 = 2$

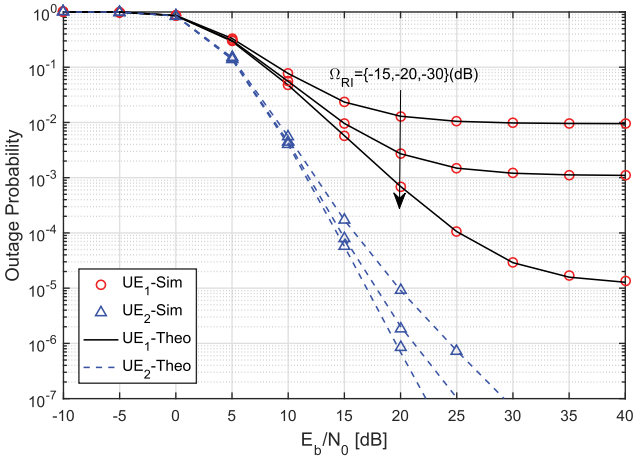

Figure 2. Outage probability versus the transmit E_b/N_0 for different values of residual SI.

signal directly. Note that from the analytical expression (9) the values of ε need to satisfy the condition $\varepsilon\gamma_{th1} < \frac{a_1}{a_2}$ for success decoding at UE_1 as shown in Section III.

Figure 4 plots ergodic capacities as a function of E_b/N_0 for different values of the power allocation coefficients when $a_1 = 0.2$, $a_2 = 0.8$ and $a_1 = 0.3$, $a_2 = 0.7$. Ergodic sum capacity is defined as the total of the ergodic capacity of UE_1 and UE_2. As shown in the figure, the analytic curves of two users obtained from (15) and (18) match perfectly with the simulated ones. The theoretical result for the ergodic sum capacity also coincides with the simulation result. These observations again confirm our analysis. It can be seen that when a_1 increases, the ergodic capacity of UE_1 improves while that of UE_2 decreases; but the ergodic sum capacity remains almost unchanged. Consequently, we can change the value of the power allocation coefficients to adjust the ergodic capacities of UE_1 and UE_2.

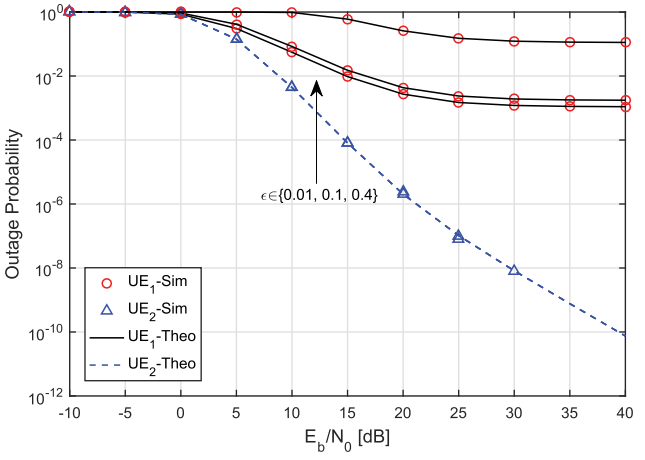

Figure 3. Outage probability of users versus the transmit E_b/N_0 for different values of ε.

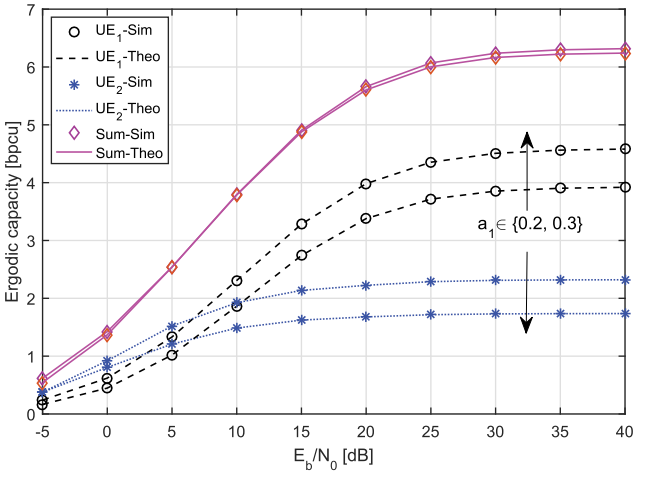

Figure 4. Ergodic capacity versus the transmit E_b/N_0 when $a_1 = 0.2, 0.3$.

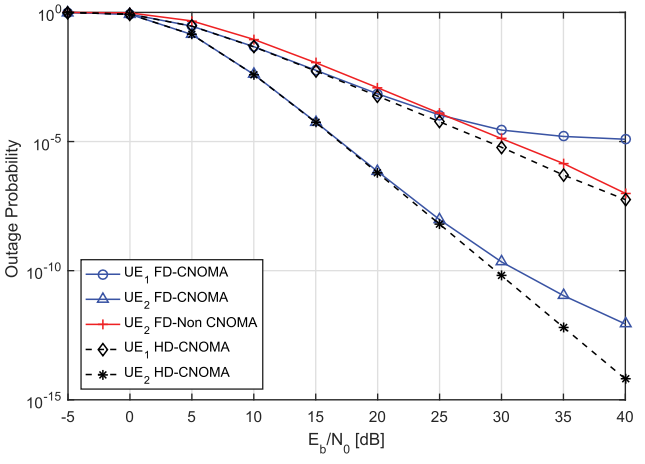

Figure 5. Outage probability of FD-C-NOMA, FD-NC-NOMA and HD-C-NOMA systems versus the transmit E_b/N_0 with $\Omega_{\text{RI}} = -30$ dB.

Figure 5 compares the outage probability of the FD-C-NOMA, FD-NC-NOMA and HD-C-NOMA systems under the constraint of $\Omega_{\text{RI}} = -30$ dB with the same parameters used in Table 1. As can be observed from the figure, the performance of UE_2 of the FD-C-NOMA system is greatly improved, and achieves a gain of 1.8–2 times in terms of power compared to the FD-NC-NOMA system in the low E_b/N_0 region, i.e [0 dB – 25 dB]. On other hand, this performance is nearly equivalent to that of UE_1 in the HD-C-NOMA system, which also proves the fairness of the NOMA principle. The system outage probability of FD-C-NOMA equivalent to that of HD-C-NOMA in the low SNR regime due to the fact that the residual SI effect is negligible. Nevertheless, in the high E_b/N_0 regime, the outage probability of the FD scheme is much worse than that of the HD scheme. Thus, SI mitigation techniques are always a top concern for FD systems to maintain a required performance.

Similarly, Figure 6 illustrates how the imperfect SIC factor affects the capacity of FD-C-NOMA, FD-NC-NOMA and HD-C-NOMA. It is clear that when ε increases, the ergodic sum capacities of these systems decrease dramatically. For instance, as can be seen at SNR = 25 dB, they decrease from about 6.0 bpcu down to 2.7 bpcu for the FD-C-NOMA and FD-NC-NOMA systems and from 3.0 bpcu down to 1.3 bpcu for the HD-C-NOMA one when the value of ε reduces from 0.4 to 0.01.

Figure 7 compares the ergodic sum capacities of the FD-C-NOMA system, FD-NC-NOMA and the HD-C-NOMA one for different values of Ω_{RI}. It can be seen from the figure that the residual SI does not affect the ergodic capacity of the HD-NOMA system, but it reduces that of the FD-C-NOMA and FD-NC-NOMA significantly. It is worth noting that the FD-C-NOMA system can double its ergodic capacity compared with the HD-C-NOMA under low residual SI level such as $\Omega_{\text{RI}} = -30$ dB. This observation is inline with that explored in the previous studies about the ability to double the spectral efficiency of the FD-C-NOMA systems (Sabharwal et al., 2014) (Debaillie et al., 2015). The results shown in Figure 7 indicate that the capacity of FD-C-NOMA and FD-NC-NOMA systems is equivalent, except that the FD-C-NOMA system capacity is slightly larger than the FD-NC-NOMA

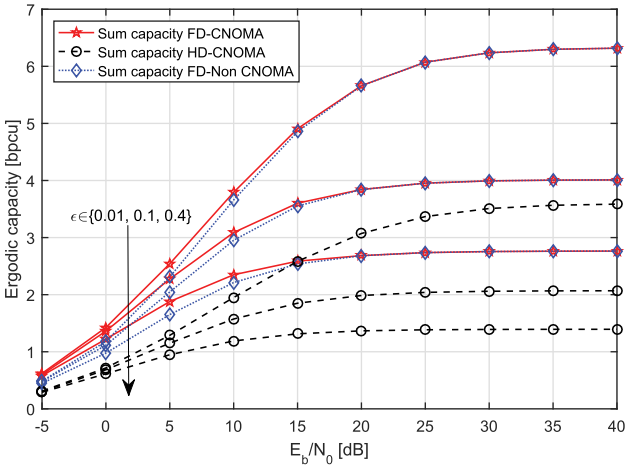

Figure 6. Ergodic sum capacity of FD-C-NOMA, FD-NC-NOMA and HD-C-NOMA systems for different values of ε.

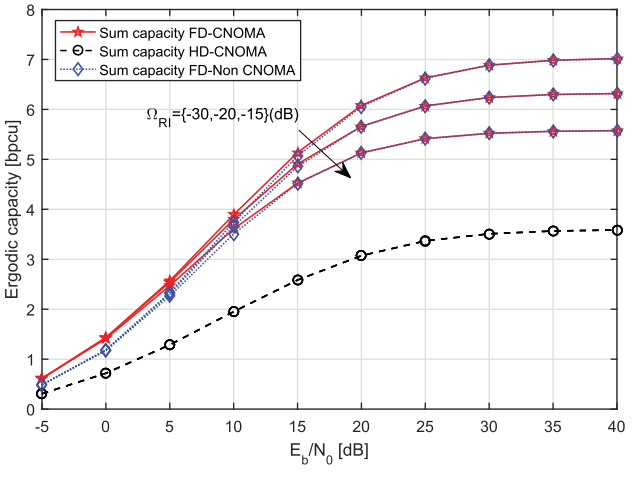

Figure 7. Ergodic sum capacity of FD-C-NOMA, FD-NC-NOMA and HD-C-NOMA systems.

system in the low E_b/N_0 region. This is due to the fact that the effect of residual SI is negligible in this region, UE_2 receives data through the relay link that has a higher SINR than the direct link.

5. Conclusions

Investigating the effects of residual SI and MAI plays an important role in the practical aspects of wireless networks implementing the FD and NOMA techniques. In this paper, we have derived the exact expressions of the outage performance and ergodic capacity for the FD-C-NOMA system under the impacts of these factors over the Nakagami-*m* fading channels. Besides, the performance of the FD-C-NOMA system has been benchmarked with that of the HD-C-NOMA and FD-NC-NOMA ones. It was understood that

the FD-C-NOMA system can achieve double ergodic sum capacity of the HD-C-NOMA and have significantly improved outage probability over the FD-NC-NOMA system. Thus, the combined FD and NOMA systems have potential applications for implementation in the future wireless networks. However, in order to attain the desired performance it is necessary to limit the impacts of the imperfect self-interference suppression and MAI.

Disclosure statement

The authors declare that they have no conflict of interest.

ORCID

Xuan Nam Tran http://orcid.org/0000-0001-8530-9354

References

Amin, O., & Lampe, L. (2012). Opportunistic energy efficient cooperative communication. *IEEE Wireless Communications Letters*, *1*(5), 412–415. https://doi.org/10.1109/WCL.2012.061212.120206

Bagwari, A., Kanti, J., & Tomar, G. S. (2015). Novel spectrum detector for IEEE 802.22 wireless regional area network. *International Journal of Smart Device and Appliance*, *3*(2), 9–25. https://doi.org/10.21742/ijsda.2015.3.2.02

Bagwari, A., & Tomar, G. S. (2013). Comparison between adaptive double-threshold based energy detection and cyclostationary detection technique for cognitive radio networks. In *Proceedings of the 2013 5th International Conference and Computational Intelligence and Communication Networks, Mathura, India* (pp. 182–185).

Bagwari, A., & Tomar, G. S. (2014). Cooperative spectrum sensing in multiple energy detectors based cognitive radio networks using adaptive double-threshold scheme. *International Journal of Electronics*, *101*(11), 1546–1558. https://doi.org/10.1080/00207217.2014.880953

Bagwari, A., & Tomar, G. S. (2015). Enriched the spectrum sensing performance of estimated SNR based detector in cognitive radio networks. *International Journal of Hybrid Information Technology*, *8*(9), 143–156. https://doi.org/10.14257/ijhit.2015.8.9.15

Bharadia, D., McMilin, E., & Katti, S. (2013). Full duplex radios. In *Proceedings of the ACM SIGCOMM 2013 conference on SIGCOMM, Hong Kong, China* (pp. 375–386).

Chen, X., Liu, G., Ding, Z., Yu, F. R., & Fan, P. (2017). Power allocation for full- duplex cooperative non-orthogonal multiple access systems. In *Proceedings of the 2017 IEEE Global Communications Conference, Singapore.* (pp. 1–6).

Chen, Y., Wang, L., and Jiao, B. (2017). Cooperative multicast non-orthogonal multiple access in cognitive radio. In *Proceedings of the 2017 nternational Conference on Communications (ICC)*. (pp. 1–6)., Paris. https://doi.org/10.1109/ICC.2017.7996607.

Chu, T. M. C., & Zepernick, H.-J. (2018). Performance of a non-orthogonal multiple access system with full-duplex relaying. *IEEE Communications Letters*, *22*(10), 2084–2087. https://doi.org/10.1109/LCOMM.2018.2852308

Debaillie, B., van Liempd, B., Hershberg, B., Craninckx, J., Rikkinen, K., van den Broek, D.-J., … Nauta, B. (2015). In-band full-duplex transceiver technology for 5G mobile networks. In *Proceedings of the 2015-41st European Solid-State Circuits Conference (ESSCIRC), Graz, Austria* (pp. 84–87).

Ding, Z., Liu, Y., Choi, J., Sun, Q., Elkashlan, M., Poor, H. V. (2017). Application of non-orthogonal multiple access in LTE and 5G networks. *IEEE Communica- tions Magazine*.

Ding, Z., Peng, M., & Poor, H. V. (2015). Cooperative non-orthogonal multiple access in 5G systems. *IEEE Communications Letters*, *19*(8), 1462–1465. https://doi.org/10.1109/LCOMM.2015.2441064

Goldsmith, A. (2005). *Wireless communications*. Cambridge University Press.
Gradshteyn, I. S., & Ryzhik, I. M. (2014). *Table of integrals, series, and products*. Academic Press.
Higuchi, K., & Benjebbour, A. (2015). Non-orthogonal multiple access (NOMA) with successive interference cancellation for future radio access. *IEICE Transactions on Communications*, *98*(3), 403–414. https://doi.org/10.1587/transcom.E98.B.403
Hoang, T. M., Tan, N. T., Hoang, N. H., & Hiep, P. T. (2018). Performance analysis of decode-and-forward partial relay selection in NOMA systems with RF energy harvesting. *Wireless Networks*, 25(8), 4585-4595. https://doi.org/10.1007/s11276-018-1746-8
Hoang, T. M., Van Son, V., Dinh, N. C., & Hiep, P. T. (2018). Optimizing duration of energy harvesting for downlink NOMA full-duplex over Nakagami-*m* fading channel. *AËU-International Journal of Electronics and Communications*, *95*, 199–206. https://doi.org/10.1016/j.aeue.2018.08.020
Islam, S. R., Avazov, N., Dobre, O. A., & Kwak, K.-S. (2017). Power-domain non- orthogonal multiple access (NOMA) in 5G systems: potentials and challenges. *IEEE Communications Surveys & Tutorials*, *19*(2), 721–742. https://doi.org/10.1109/COMST.2016.2621116
Kim, J.-B., Lee, I.-H., & Lee, J. (2018). Capacity scaling for D2D aided cooperative relaying systems using NOMA. *IEEE Wireless Communications Letters*, *7*(1), 42–45. https://doi.org/10.1109/LWC.2017.2752162
Le, T. T. H., & Tran, X. N. 2019. Performance analysis of repeated index modulation with coordinate interleaving over Nakagami-*m* fading channel. *Research and Development on Information and Communication Technology*. Retrieved from 2019(1), 23–30. https://doi.org/10.32913/mic-ict-research.v2019.n1.863
Lee, S. (2018 12). Cooperative non-orthogonal multiple access for future wireless communications. *EAI Endorsed Transactions on Industrial Networks and Intelligent Systems*, *5*(17), 17. https://doi.org/10.4108/eai.19-12-2018.156078
Li, Y., Sun, K., & Cai, L. (2018). Cooperative device-to-device communication with network coding for machine type communication devices. *IEEE Transactions on Wireless Communications*, *17*(1), 296–309. https://doi.org/10.1109/TWC.2017.2765306
Liu, K. R., Sadek, A. K., Su, W., & Kwasinski, A. (2009). *Cooperative communications and networking*. Cambridge University Press.
Luo, F.-L., & Zhang, C. (2016). *Signal processing for 5G: Algorithms and implementations*. John Wiley & Sons.
Nguyen, L. V., Nguyen, B. C., Tran, X. N., & Le, T. D. (2019). Closed-form expression for the symbol error probability in full-duplex spatial modulation relay system and its application in optimal power allocation. *Sensors*, *19*(24), 5390. https://doi.org/10.3390/s19245390
Nguyen, -X.-X., & Do, D.-T. (2019). Syste*m* performance of cooperative NOMA with Full-Duplex relay over Nakaga*m*i-*m* fading channels. *Mobile Information Systems* 2019. 1-12 https://doi.org/10.1155/2019/7547431
Nwankwo, C. D., Zhang, L., Quddus, A., Imran, M. A., & Tafazolli, R. (2017). A survey of self-interference management techniques for single frequency full duplex systems. *IEEE Access*, *6*, 30242–30268. https://doi.org/10.1109/ACCESS.2017.2774143
Sabharwal, A., Schniter, P., Guo, D., Bliss, D. W., Rangarajan, S., & Wichman, R. (2014). In-band full-duplex wireless: challenges and opportunities. *IEEE Journal on Selected Areas in Communications*, *32*(9), 1637–1652. https://doi.org/10.1109/JSAC.2014.2330193
Shamganth, K., & Sibley, M. J. (2017). A survey on relay selection in cooperative device-to-device (D2D) communication for 5G cellular networks. In *Proceesings of the 2017 international conference on energy, communication, data analytics and soft computing (icecds), Chennai, Tamil Nadu, India* (pp. 42–46).
Shankar, P. M. (2017). *Fading and shadowing in wireless systems*. Springer.
Toka, M., & Kucur, O. (2018). Performance of antenna selection schemes in dual hop full-duplex decode-and-forward relaying over Nakagami-*m* fading channels. *AËU-International Journal of Electronics and Communications*, *86*, 92–102. https://doi.org/10.1016/j.aeue.2018.01.018.
Wan, D., Wen, M., Ji, F., Yu, H., & Chen, F. (2018). Non-orthogonal multiple access for cooperative communications: Challenges, opportunities, and trends. *IEEE Wireless Communications*, *25*(2), 109–117. https://doi.org/10.1109/MWC.2018.1700134

Yue, X., Liu, Y., Kang, S., & Nallanathan, A. (2017). Performance analysis of NOMA with fixed gain relaying over Nakagami-*m* fading channels. *IEEE Access*, *5*, 5445–5454. https://doi.org/10.1109/ACCESS.2017.2677504

Yue, X., Liu, Y., Kang, S., Nallanathan, A., & Ding, Z. (2018). Exploiting full/half- duplex user relaying in NOMA systems. *IEEE Transactions on Communications*, *66*(2), 560–575. https://doi.org/10.1109/TCOMM.2017.2749400

Zhang, L., Liu, J., Xiao, M., Wu, G., Liang, Y.-C., & Li, S. (2017). Performance analysis and optimization in downlink NOMA systems with cooperative full- duplex relaying. *IEEE Journal on Selected Areas in Communications*, *35*(10), 2398–2412. https://doi.org/10.1109/JSAC.2017.2724678

Zhang, Z., Ma, Z., Xiao, M., Ding, Z., and Fan, P. (2017). Full-duplex device-to-device-aided cooperative nonorthogonal multiple access. *IEEE Transactions on Vehicular Technology*, *66*(4), 4467–4471. https://doi.org/10.1109/TVT.2016.2600102

Zhang, Z., Chai, X., Long, K., Vasilakos, A. V., & Hanzo, L. (2015). Full duplex techniques for 5G networks: Self-interference cancellation, protocol design, and relay selection. *IEEE Communications Magazine*, *53*(5), 128–137. https://doi.org/10.1109/MCOM.2015.7105651

Zhong, C., & Zhang, Z. (2016). Non-orthogonal multiple access with cooperative full-duplex relaying. *IEEE Communications Letters*, *20*(12), 2478–2481. https://doi.org/10.1109/LCOMM.2016.2611500

Appendix A: Proof of Theorem 1

Expression (8) can be rewritten as

$$\mathrm{OP}_1 = 1 - \Pr\Big(|h_1|^2\rho(a_2 - a_1\gamma_{\mathrm{th}2}) > \gamma_{\mathrm{th}2}\Big(|h_{\mathrm{RI}}|^2\rho + 1\Big),$$

$$|h_1|^2\rho(a_1 - a_2\varepsilon\gamma_{\mathrm{th}1}) > \gamma_{\mathrm{th}1}\Big(|h_{\mathrm{RI}}|^2\rho + 1\Big)\Big). \tag{31}$$

Case 1: When $\frac{a_1}{a_2} \geq \frac{1}{\gamma_{\mathrm{th}2}}$ or $\frac{a_1}{a_2} \leq \varepsilon\gamma_{\mathrm{th}1}$, it is easy to see that $\Pr(\gamma_{12} > \gamma_{\mathrm{th}2}, \gamma_{11} > \gamma_{\mathrm{th}1}) = 0$. Thus, the outage probability of UE_1 is equal to one, i.e, $\mathrm{OP}_1 = 1$.

Case 2: When $\varepsilon\gamma_{\mathrm{th}1} \leq \frac{a_1}{a_2} \leq \frac{\gamma_{\mathrm{th}1}(1+\varepsilon\gamma_{\mathrm{th}2})}{\gamma_{\mathrm{th}2}(1+\gamma_{\mathrm{th}1})}$, according to the theory of conditional probability (Gradshteyn & Ryzhik, 2014), expression (8) is derived as follows

$$\mathrm{OP}_1 = 1 - \Pr\Big(|h_1|^2 > b_1\Big(|h_{\mathrm{RI}}|^2\rho + 1\Big)\Big)$$

$$= 1 - \int_0^{\infty}\Big[1 - F_{|h_1|^2}(b_1(z\rho + 1))\Big]f_{|h_{\mathrm{RI}}|^2}(z)dz, \tag{32}$$

where $b_1 = \frac{\gamma_{th1}}{\rho(a_1 - a_2\varepsilon\gamma_{th1})}$, $f_{|h_{\mathrm{RI}}|^2}(z)$ denotes the PDF of the Rayleigh distribution for variable $|h_{\mathrm{RI}}|^2$, and $F_{|h_1|^2}(.)$ is its associated cumulative distribution function (CDF) which has the Gamma distribution. As (Shankar, 2017), they are expressed, respectively, as follows

$$f_{|h_{\mathrm{RI}}|^2}(z) = \frac{1}{\Omega_{\mathrm{RI}}}e^{-\frac{z}{\Omega_{\mathrm{RI}}}} \tag{33}$$

$$F_{|h_1|^2}(b_1(z\rho + 1)) = 1 - \frac{1}{\Gamma(m_1)}\Gamma\Big(m_1, (b_1(z\rho + 1)\frac{m_1}{\Omega_1}\Big), \tag{34}$$

where $\Gamma(.)$, $\Gamma(.,.)$ are, respectively, the Gamma function and incomplete Gamma function determined as in (Gradshteyn & Ryzhik, 2014).

Substituting (33) and (34) into (32), OP_1 is rewritten as follows

$$\mathrm{OP}_1 = 1 - \frac{1}{\Omega_{\mathrm{RI}}} e^{-\frac{m_1\varphi}{\Omega_1}} \sum_{k=0}^{m_1-1} \left(\frac{m_1\varphi}{\Omega_1}\right)^k \frac{1}{k!}$$

$$\times \int_0^{\infty} (z\rho + 1)^k e^{-\frac{m_1 b_1 \rho z}{\Omega_1} - \frac{z}{\Omega_{\mathrm{RI}}}} dz. \tag{35}$$

Based on (Gradshteyn & Ryzhik, 2014, eq.(1.111)), the probability is simplified to

$$\mathrm{OP}_1 = 1 - \frac{1}{\Omega_{\mathrm{RI}}} e^{-b_1} \sum_{k=0}^{m_1-1} \frac{b_1^k}{k!} \sum_{t=0}^{k} \rho^t \binom{k}{t} \int_0^{\infty} z^t e^{-b_1\rho z - \frac{z}{\Omega_{\mathrm{RI}}}} dz. \tag{36}$$

Thanks to the help of (Gradshteyn & Ryzhik, 2014, eq.(3.351.3)), after some manipulations, the closed-form expression of OP_1 is obtained as the second expression into (9).

Case 3: When $\frac{\gamma_{th1}(1+\varepsilon\gamma_{th2})}{\gamma_{th2}(1+\gamma_{th1})} \le \frac{a_1}{a_2} \le \frac{1}{\gamma_{th2}}$, calculating outage probability OP_1 can be done similarly to the previous case with a being replaced by $b_2 = \frac{\gamma_{\mathrm{th2}}}{\rho(a_2 - a_1\gamma_{\mathrm{th2}})}$. We then obtain the result as the third expression in (9).

Combining the proofs for the above three cases, Theorem 1 is thus proved.

Appendix B: Proof of Theorem 2

From (11) and (12) expressions, the outage probability of UE_2 can be written as

$$OP_2 = \Pr[\max\{\min(\gamma_{12}, \gamma_{2R}), \gamma_{2S}\} \le \gamma_{\mathrm{th2}}]. \tag{37}$$

Due to the assumption of independent channels, expression (37) can be derived as follows

$$OP_2 = \Pr(\min(\gamma_{12}, \gamma_{2R}) \le \gamma_{\mathrm{th2}}) \Pr(\gamma_{2S} \le \mathrm{g}_{\mathrm{th2}})\gamma,$$

$$= [1 - \Pr(\gamma_{12} > \gamma_{\mathrm{th2}}) \Pr(\gamma_{2R} > \gamma_{\mathrm{th2}})] \times \Pr(\gamma_{2S} \le \gamma_{\mathrm{th2}}). \tag{38}$$

By calculating the subexpression of (38), the probability $\Pr(\gamma_{12} > \gamma_{\mathrm{th2}})$ can be obtained as follows

$$\Pr(\gamma_{12} > \gamma_{\mathrm{th2}}) = 1 - \Pr\left(|h_1|^2 \ge b_2\left(|h_{\mathrm{RI}}|^2\rho + 1\right)\right)$$

$$= 1 - \int_0^{\infty} \left[1 - F_{|h_1|^2}(b_2(z\rho + 1))\right] \times f_{|h_{\mathrm{RI}}|^2}(z)dz. \tag{39}$$

Substituting $F_{|h_1|^2}(.)$ and $f_{|h_{\mathrm{RI}}|^2}(z)dz$ into (39), and then using the CDF of $|h_0|^2$, $|h_2|^2$, the probabilities in (38) can be further expressed as

$$\Pr(\gamma_{12} > \gamma_{\mathrm{th2}}) = \frac{1}{\Omega_{\mathrm{RI}}} e^{-b_2} \sum_{k=0}^{m_1-1} \sum_{t=0}^{k} \frac{b_2^k}{k!} \times \binom{k}{t} \rho^t t! \left(b_2\rho + \frac{1}{\Omega_{\mathrm{RI}}}\right), \tag{40}$$

$$\Pr(\gamma_{2R} > \gamma_{\mathrm{th2}}) = 1 - \Pr\left(|h_2|^2 \le \frac{\gamma_{\mathrm{th2}}}{\rho}\right) = \frac{1}{\Gamma(m_2)} \Gamma\left(m_2, \frac{m_2\gamma_{\mathrm{th2}}}{\rho\Omega_2}\right), \tag{41}$$

$$\Pr(\gamma_{2S} \le \gamma_{\mathrm{th2}}) = \Pr\left(|h_0|^2 \le b_2\right) = 1 - \frac{1}{\Gamma(m_0)} \Gamma\left(m_0, \frac{m_0 b_2}{\Omega_0}\right). \tag{42}$$

Substituting (40), (41) and (42) into (38), we have the closed-form expression of OP_2 as in (13).

Appendix C: Proof of Theorem 3

From expression (14), $\bar{C}_1$ can be rewritten as

$$\bar{C}_1 = \mathrm{E}\left[\log\left(1+|h_1|^2(a_1+a_2\varepsilon)\rho+|h_{\mathrm{RI}}|^2\rho\right)\right] - \mathrm{E}\left[\log\left(1+|h_1|^2 a_2\varepsilon\rho+|h_{\mathrm{RI}}|^2\rho\right)\right]. \tag{43}$$

Let us define $X = |h_1|^2(a_1+a_2\varepsilon)\rho+|h_{\mathrm{RI}}|^2\rho$ and $Y = |h_1|^2(a_1+a_2\varepsilon)\rho+|h_{\mathrm{RI}}|^2\rho$, we can obtain the ergodic capacity at UE_1 as follows

$$\bar{C}_1 = \frac{1}{\ln 2}\left(\underbrace{\int_0^\infty \frac{1-F_X(x)}{1+x}dx}_{\mathrm{I}_1} - \underbrace{\int_0^\infty \frac{1-F_Y(y)}{1+y}dy}_{\mathrm{I}_2}\right), \tag{44}$$

where $F_X(x)$, $F_Y(y)$ are the CDFs of X and Y respectively. We now analyse each of these expressions.

First, $F_X(x)$ is expressed as follows

$$\begin{aligned} F_X(x) &= \Pr\left(|h_1|^2 < \tfrac{x-|h_{\mathrm{RI}}|^2\rho}{(a_1+a_2\varepsilon)\rho}\right) \\ &= \int_0^{\frac{x}{\rho}} F_{|h_1|^2}\left(\tfrac{x-z\rho}{(a_1+a_2\varepsilon)\rho}\right) f_{|h_{\mathrm{RI}}|^2}(z)dz. \end{aligned} \tag{45}$$

Substituting expressions of $f_{|h_{\mathrm{RI}}|^2}(z)$ and $F_{|h_1|^2}(.)$, $F_X(x)$ can be calculated as

$$\begin{aligned} F_X(x) &= \int_0^{\frac{x}{\rho}}\left[1-e^{-\frac{m_1(x-z\rho)}{\Omega_1(a_1+a_2\varepsilon)\rho}}\sum_{k=0}^{m_1-1}\times\left(\frac{m_1(x-z\rho)}{\Omega_1(a_1+a_2\varepsilon)\rho}\right)^k\frac{1}{k!}\right]\frac{1}{\Omega_{\mathrm{RI}}}e^{-\frac{z}{\Omega_{\mathrm{RI}}}}dz \\ &= \frac{1}{\Omega_{\mathrm{RI}}}\int_0^{\frac{x}{\rho}}e^{-\frac{z}{\Omega_{\mathrm{RI}}}}dz - \frac{1}{\Omega_{\mathrm{RI}}}e^{-b_{11}x}\sum_{k=0}^{m_1-1}\frac{b_{11}^k}{k!}\times\int_0^{\frac{x}{\rho}}e^{b_{11}\rho z-\frac{z}{\Omega_{\mathrm{RI}}}}(x-\rho z)^k dz \\ &= 1-e^{-\frac{x}{\rho\Omega_{\mathrm{RI}}}} - e^{-\frac{b_{11}}{\Omega_{\mathrm{RI}}}}\sum_{k=0}^{m_1-1}\sum_{t=0}^{k}\frac{b_{11}^k}{k!}\times\binom{k}{t}(-1)^t x^{k-t}\rho^t\int_0^{\frac{x}{\rho}}z^t e^{-c_{11}z}dz, \end{aligned} \tag{46}$$

Next, we calculate I_1 in the following two cases.

- Case 1: $c_{11}\neq 0$.

Using the following identities $\int_0^{\frac{x}{\rho}} z^t e^{-c_{11}\rho z}dz = c_{11}^{-t-t}\gamma\left(t+1,\frac{c_{11}x}{\rho}\right)$ in (Gradshteyn & Ryzhik, 2014, eq. (3.381.1)) and $\gamma\left(t+1,\frac{c_{11}x}{\rho}\right) = t!\left[1-e^{-\frac{c_{11}x}{\rho}}\sum_{m=0}^{t}\left(\frac{c_{11}x}{\rho}\right)^m\frac{1}{m!}\right]$ in (Gradshteyn & Ryzhik, 2014, eq. (8.352.6)) for $F_X(x)$, I_1 can be expressed as

$$\mathrm{I}_1 = \int_0^\infty\frac{e^{-\frac{x}{\rho\Omega_{\mathrm{RI}}}}}{1+x}dx + \frac{1}{\Omega_{\mathrm{RI}}}\sum_{k=0}^{m_1-1}\sum_{t=0}^{k}\frac{b_{11}^k}{k!}\binom{k}{t}\times\frac{(-1)^t\rho^t t!}{c_{11}^{t+1}}\left[\int_0^\infty\frac{e^{-b_{11}x}x^{k-t}}{1+x}dx - \sum_{q=0}^{t}\left(\frac{c_{11}}{\rho}\right)^q \times\frac{1}{q!}\int_0^\infty\frac{e^{-\left(b_{11}+\frac{c_{11}}{\rho}\right)x}x^{k-t+q}}{1+x}dx\right], \tag{47}$$

Thanks to the help of (Gradshteyn & Ryzhik, 2014, eq.(3.383.10)), I_1 is given by the first expression of (16).

- Case 2: $c_{11}=0$. $F_X(x)$ is calculated as

$$F_X(x) = 1-e^{-\frac{x}{\rho\Omega_{\mathrm{RI}}}} - e^{-\frac{b_{11}}{\Omega_{\mathrm{RI}}}}\sum_{k=0}^{m_1-1}\sum_{t=0}^{k}\frac{b_{11}^k}{k!}\times\binom{k}{t}\frac{(-1)^t x^{k+1}}{(t+1)\rho}. \tag{48}$$

Substituting (48) into (44), we can obtain I_1 as follows

$$\mathrm{I}_1 = \int_0^{\infty} \frac{e^{-\frac{x}{\rho\Omega_{\mathrm{RI}}}}}{1+x} dx + \frac{1}{\Omega_{\mathrm{RI}}} \sum_{k=0}^{m_1-1} \sum_{t=0}^{k} \frac{b_{11}^k}{k!} \binom{k}{t} \times \frac{(-1)^t}{(t+1)\rho} \int_0^{\infty} \frac{\mathrm{e}^{-b_{11}x} x^{k+1}}{1+x} dx. \tag{49}$$

Using (Gradshteyn & Ryzhik, 2014, eq.(3.383.10)), we can obtain the second expression of (16).

Now, we consider $F_Y(y)$ expressed as follows

$$F_Y(y) = \Pr\left(|h_1|^2 < \frac{y - |h_{\mathrm{RI}}|^2\rho}{a_2\varepsilon\rho}\right)$$

$$= \int_0^{\frac{y}{\rho}} F_{|h_1|^2}\left(\frac{y - z\rho}{a_2\varepsilon\rho}\right) f_{|h_{\mathrm{RI}}|^2}(z) dz. \tag{50}$$

Similar to I_1, we can calculate I_2 as given in (16). The proof is thus completed.